Inorganica Chimica Acta 471 (2018) 272–279

Contents lists available at ScienceDirect

Inorganica Chimica Acta

journal homepage: www.elsevier.com/locate/ica

Research paper

Magnetic properties of the anion-radical salts $[M(bipy)_3](TCNQ)_4 \cdot X$, where M = Co, Ni, Zn and X = H_2O or $(CH_3)_2CO$

D. Šoltésová [a,*], G. Vasylets [b], E. Čižmár [a], A.V. Fedorchenko [a,1], V. Starodub [c], V. Medviediev [d], O. Shishkin [e], O. Bukrynov [b], A. Feher [a]

[a] Institute of Physics, Faculty of Science, P. J. Šafárik University, Park Angelinum 9, 041 54 Košice, Slovakia
[b] Applied Chemistry Department, V. N. Karazin Kharkiv National University, Svobody Sq. 4, 61022 Kharkiv, Ukraine
[c] Institute of Chemistry, Jan Kochanowski University, Świętokrzyska 15G, 25-406 Kielce, Poland
[d] Institute of Low Temperature and Structure Research, Polish Academy of Sciences, Okólna Str. 2, P.O. Box 1410, 50-950 Wrocław, Poland
[e] SSI "Institute for Single Crystals", National Academy of Science of Ukraine, Nauky Ave. 60, 61001 Kharkiv, Ukraine

ARTICLE INFO

Article history:
Received 22 June 2017
Received in revised form 23 September 2017
Accepted 3 November 2017
Available online 7 November 2017

Keywords:
Anion-radical salt
Magneto-structural correlations
Metal–radical interaction

ABSTRACT

An anion-radical salt (ARS) $[Co(bipy)_3](TCNQ)_4 \cdot H_2O$ was synthesized and its crystal structure was resolved. The experimental investigation of $[Co(bipy)_3](TCNQ)_4 \cdot H_2O$ and two ARS with similar crystal structure $[Zn(bipy)_3](TCNQ)_4 \cdot H_2O$ and $[Ni(bipy)_3](TCNQ)_4 \cdot (CH_3)_2CO$ by the measurement of the temperature dependence of magnetic susceptibility at temperature from 1.8 K to 300 K, the field dependence of magnetization up to 7 T at different temperatures and EPR spectra in temperature range from 2 K to 300 K was performed. $[Zn(bipy)_3](TCNQ)_4 \cdot H_2O$ was used to estimate the contribution of the TCNQ radicals to the magnetic moment. In result, the compound $[Co(bipy)_3](TCNQ)_4 \cdot H_2O$ was characterized by the presence of Co^{2+} ions in spin-admixed state and low-temperature susceptibility, magnetization and specific heat of $[Ni(bipy)_3](TCNQ)_4 \cdot (CH_3)_2CO$ was shown to be dominated by the contribution of single-ion anisotropy of Ni^{2+} ions.

1. Introduction

Charge-transfer compounds have a rich history dating back to the early 1970s, and presently, they are receiving renewed attention due to their emerging role in applications [1,2]. For example, 7,7,8,8-tetracyanoquinodimethane (TCNQ) molecules are one example of organic anion-radical salts (ARS) that possess a wide range of magnetic, electrical, and optical properties. The additional incorporation of metal ions in ARS compounds leads to materials combining the properties of organic and inorganic components for use in various applications, including nanoelectronics [2] and quantum-computing [3,4]. More specifically, ARS complexes based on TCNQ can form low-dimensional magnets, and many of them form dimerized magnetic systems with alternating exchange interactions. It is particularly noteworthy that small modifications of the crystal structure have considerable impact on their charge transfer and magnetic properties [5–8]. This intimate "form-function" correlation between crystal structure and exchange interaction between anion radicals and transition metal ions have been investigated in ARS based on TCNQ containing transition metal ions [9,10]. Recently, ARS $[Mn(phen)_3](TCNQ)_2 \cdot H_2O$ and $[Co(phen)_3](TCNQ)_2 \cdot H_2O$ were studied and a weak interaction was found between the TCNQ anion-radicals and transition metal ions [11].

The present work was initiated to explore the magnetic and thermodynamic properties of $[Ni(bipy)_3](TCNQ)_4 \cdot (CH_3)_2CO$, whose structural properties were already reported [12]. In order to better understand the magnetic response arising from the Ni^{2+} ion, $[Zn(bipy)_3](TCNQ)_4 \cdot H_2O$ [12] was magnetically characterized. In addition, in an attempt to expand the transition metal ions being incorporated in these types of complexes, $[Co(bipy)_3](TCNQ)_4 \cdot H_2O$ was synthesized for the first time, and its structural and magnetic properties are reported herein. The magnetic characterization of each complex involved temperature-dependent and isothermal magnetic-field dependent magnetometry and temperature-dependent X-band (9.4 GHz) electron paramagnetic resonance (EPR). The thermodynamic response of $[Ni(bipy)_3](TCNQ)_4 \cdot (CH_3)_2CO$ was also studied by specific heat techniques. Briefly stated, the magnetic response of $[Co(bipy)_3](TCNQ)_4 \cdot H_2O$ is characterized by the presence of Co^{2+} ions in a spin-admixed state, while the magnetic

---

* Corresponding author.
E-mail address: daniela.soltesova@student.upjs.sk (D. Šoltésová).

[1] Coming from B.Verkin Institute for Low Temperature Physics and Engineering of NAS of Ukraine, Nauky av., 47, Kharkiv, Ukraine.

https://doi.org/10.1016/j.ica.2017.11.001
0020-1693/© 2017 Elsevier B.V. All rights reserved.

response of $[Ni(bipy)_3](TCNQ)_4{\cdot}(CH_3)_2CO$ is dominated by the contribution of single-ion anisotropy of Ni^{2+} ions at low-temperatures.

2. Experimental methods

The synthesis $[Zn(bipy)_3](TCNQ)_4{\cdot}H_2O$ (**1**) and $[Ni(bipy)_3](TCNQ)_4{\cdot}(CH_3)_2CO$ (**2**) followed the previously published protocols [12,13]. In fact, the samples used in this work are from the same batches as the ones used previously [12,13]. Whereas $[Co(bipy)_3](TCNQ)_4{\cdot}H_2O$ (**3**) was synthesized in the manner used for (**1**) [12], with the only exception being the transition metal starting materials.

X-ray diffraction studies were performed using an automatic "Xcalibur 3" diffractometer (graphite monochromated MoKα radiation, CCD-detector ω scanning). The structure was solved by direct method using SHELX97 package [14]. The H atoms were placed in calculated positions (with C—H and O—H distances are 0.93 Å and 0.85 Å, respectively) and refined riding on their parent atoms with $U_{iso} = nU_{eq}$ (n = 1.5 for water molecules and n = 1.2 for other hydrogen atoms). Full-matrix least-squares refinement against F2 in anisotropic approximation. Crystallographic data and parameters of structure refinement are listed in Table 1. Full set of final atomic coordinates, geometrical parameters and crystallographic data have been deposited with the Cambridge Crystallographic Data Centre. CCDC deposition number of crystal structure of (**3**) is 1536913. These data can be obtained free of charge from the Cambridge Crystallographic Data Centre via www.ccdc.cam.ac.uk/products/csd/request/.

Measurements of magnetic response were performed in a commercial Quantum Design MPMS-XL with iHelium3 option and Quantum Design MPMS3 on nascent polycrystalline samples. Temperature dependence of magnetic susceptibility, estimated as a ratio of the measured magnetic moment and applied magnetic field, of all studied compounds was investigated in magnetic field 10 mT and 100 mT in different temperature ranges, specifically, for compound (**1**) from 1.8 K to 300 K, for (**2**) from 0.46 K to 300 K and for (**3**) from 4.5 K to 300 K. The samples were packed in a clear gelatine capsule held by a plastic straw or in polypropylene VSM capsule mounted in a MPMS3 brass sample holder. The diamagnetic contribution of background (gelatine or VSM capsule) was measured in separate experiments and subtracted from the temperature dependence of raw magnetic moment. Core diamagnetic susceptibility was estimated using Pascal's constants [15] and typical temperature independent paramagnetism of transition metal ions was subtracted from the total susceptibility. The field dependence of magnetization was measured in magnetic fields up to 7 T at temperatures 1.8 K, 5 K and 15 K and for compound (**2**) in addition at temperatures 0.5 K, 0.8 K, 1.2 K and 300 K.

Temperature dependence of specific heat of (**2**) was measured on a single crystal using a Quantum Design PPMS equipped with a ^3He refrigerator in the temperature range from 0.4 K to 35 K and in magnetic fields from 0 T to 5 T. The magnetic field was applied parallel to the crystallographic *c*-axis.

The EPR spectra were investigated using Bruker ELEXSYS II E500 X-band spectrometer with operating frequency 9.4 GHz equipped with ESR910 flow-type helium cryostat. The measurements were performed in the temperature range from 2 K to 300 K. Nascent polycrystalline samples were further pulverized and mixed with Apiezon N grease and attached to the Suprasil sample holder.

The simulation of magnetic and thermodynamic properties was performed using EasySpin [16] toolbox in MATLAB [17] environment, which allows the calculation of eigenvalues of the proposed spin Hamiltonian for systems with a small number of spins by exact diagonalization method, which are then used to calculate thermodynamic and magnetic properties.

Table 1
Crystal data for (**3**).

Crystal data	
Empirical formula	$C_{78}H_{42}N_{22}CoO$
Formula weight	1362.27
Temperature/K	293(2)
Crystal system	Triclinic
Space group	$P-1$
a/Å, b/Å, c/Å	13.4119(6), 15.8507(7), 16.6125(8)
α/°, β/°, γ/°	98.026(4), 94.843(4), 95.732(4)
Volume/Å^3	3462.2(3)
Z	2
$d_{calc}/mg \times mm^{-3}$	1.307
μ/mm^{-1}	0.312
F(0 0 0)	1398
Data collection	
Reflections collected	47592
Independent reflections	15793
$2\Theta_{max}$	55°
R_{int}	0.0577
Refinement	
Parameters	937
Reflections with F > 4σ(F)	8137
R1[F2 > 2σ(F2)]	0.0577
wR^2(all data)	0.1368
S(goodness-of-fit)	0.925

3. Experimental results and discussion

3.1. Synthesis of $[Co(bipy)_3](TCNQ)_4{\cdot}H_2O$

Hot solution of $[Co(bipy)_3]I_2$ (1.5 g, 1.92 mmol) in 30 ml of acetone was added in one portion to hot solution of TCNQ in 50 ml of acetone (1.05 g, 5.12 mmol). The black solution obtained was left for 3 days in dark place. Black crystals precipitated were collected, washed with ether and dried. This gave the title compound in 55% yield (0.95 g). Elemental analysis: calc. C – 69.38%, N – 21.98%, H – 3.31%; found C – 68.70%, N – 21.45%, H – 3.35%.

3.2. The crystal structure

The crystal and molecular structures of (**1**) and (**2**) have been reported previously [12,13]. On the other hand, the structure of (**3**) (see Fig. 1) was not previously published, so it is reported here for the first time. Overall, the crystal structures of these three compounds are very similar, because these structures have the same space group, the unit cell parameters and the positions of atoms also are the similar, the structure of (**3**) will be presented here in detail.

For (**3**), the Co^{2+} ion has a slightly distorted octahedral coordination in complex cation $[Co(bipy)_3]^{2+}$ *in the lattice* (Fig. 2). The corresponding Co-N distances are within the range 2.070(2)–2.109(2) Å. A water molecule is disordered over three positions with equal populations. Asymmetric part of the unit cell contains four TCNQ anion-radicals (labelled A–D at Fig. 3). TCNQ anion-radicals cannot be differentiated in chemical bond lengths considering experimental error of the X-ray experiment. Thus, formal charge $-2\bar{e}$ is being evenly delocalized on four anion-radicals, which have hence charge about $-0.5\bar{e}$ on each. The anion-radicals form two types of stacks (chains) along [1 0 0] crystallographic axis. Both stacks contain parallel and slightly shifted TCNQ anion-radicals with respect to each other. The first stack is formed by A and B molecules (AABB type) and the second one contains C and D molecules (CCDD type) (Fig. 4).

Anion radicals in stacks have some trend to *n*-merization: with forming π-tetramers (ABBA) and π-dimers (CC and DD). The shortest C…C distances between anion radicals at stacks are: A-A – 3.49 Å; A-B – 3.32 Å; B-B – 3.35 Å; C-C – 3.25 Å, C-D – 3.42 Å and D-D –

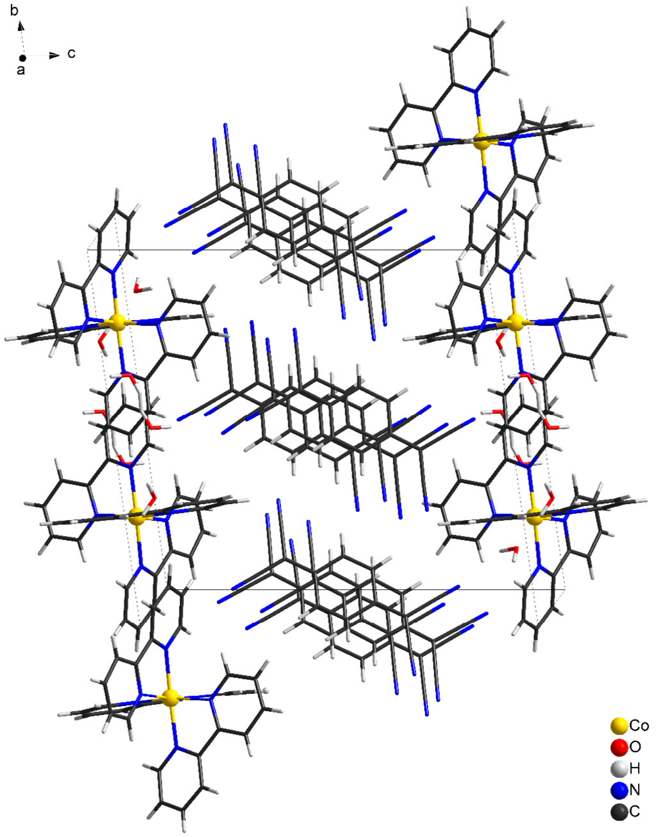

Fig. 1. Structural motif of (**3**) viewed along *a* axis.

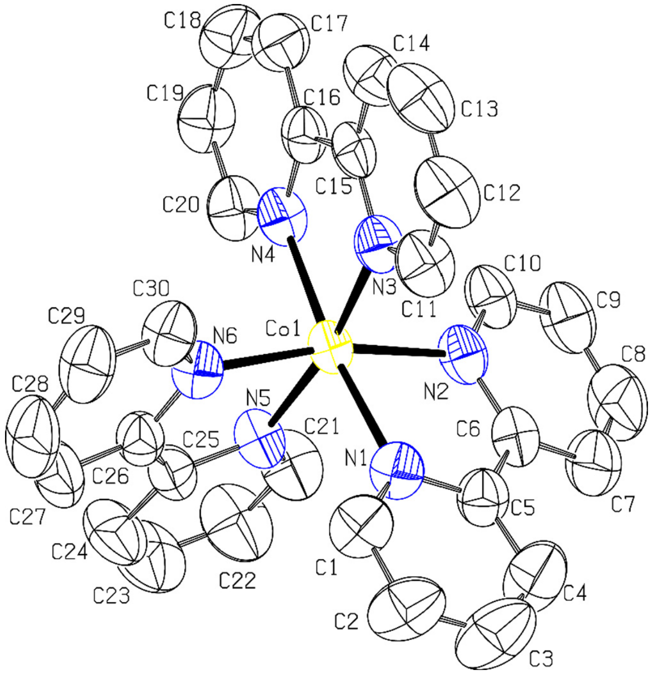

Fig. 2. Molecular structure of complex cation of compound (**3**) according to X-ray diffraction data. Thermal ellipsoids are drawn at 50% probability level. Hydrogen atoms are omitted for clarity.

3.30 Å. Also complex cation forms weak C—H—N hydrogen bond (C13-H13 – N16[i] [i: 1−x, 1−y, 2−z], H-N 2.59 Å, C—H—N 164°) with C-type anion radicals and short C–N contacts (C27–N11[j] [j: 1−x, 1−y, 1−z] 3.19 Å, van der Waals radii sum [18] 3.21 Å) with A-type of TCNQ.

3.3. Magnetic properties

3.3.1. $[Zn(bipy)_3](TCNQ)_4{\cdot}H_2O$

Magnetic susceptibility of (**1**) was investigated in the temperature range from 1.8 K to 300 K (Fig. 5). Compound (**1**) consists of Zn^{2+} ions, which are not magnetic. There the data indicate the only magnetic contribution arises from the anion-radicals TCNQ. Temperature dependence of magnetic susceptibility displays an increase with decreasing temperature in the whole temperature range. No difference was observed in measurement realized in zero-field cooled (ZFC) and field cooled (FC) regimes. The effective magnetic moment per formula unit is decreasing with decreasing temperature from the room temperature value μ_{eff} = 1.22 μ_B. The analysis of bond lengths from the X-ray crystallographic data according to Kistenmacher relationship [19] as shown in Table 2 indicates that one structural dimer of TCNQ carries effectively spin $S = 1/2$ in all studied anion-radical salts, which contain TCNQ tetramers. In such case the expected value of the effective magnetic moment of one TCNQ dimer is 1.73 μ_B. The measured value of 1.22 μ_B indicates the presence of significant antiferromagnetic (AFM) interaction between TCNQ dimers, which can lead to the total $S = 0$ state of TCNQ tetramers at low temperatures. It can be expected that dimerized spin chains may be formed due to weaker interactions between TCNQ tetramers along the chains (stacks). Subsequently, the excitation of spin dimers to spin-triplet states occurs with increasing temperature and magnetic moment increases slowly. At low temperatures only uncoupled spins (end-chain moments from chain fragments, eventually) contribute to the total susceptibility of (**1**) as paramagnetic entities. The magnetic susceptibility follows Curie law in the low-temperature range ($1.8 < T < 20$ K) with the effective value of Curie constant $C = 0.063$ emu K/mol, from which concentration of chain-end spins was estimated to be approximately x = 0.08.

In the whole temperature range, the temperature dependence of magnetic susceptibility was analysed as the sum of dimerized alternating chain formed by TCNQ anion-radicals (χ_{stacks}) [20], temperature independent contribution (χ_{Pauli}) due to semiconducting character of compound [13], which represents Pauli paramagnetism [21], and contribution of uncoupled spins (χ_{para}):

$$\chi = (1 - x)\chi_{stacks} + \chi_{Pauli} + x\chi_{para} \qquad (1)$$

with resulting parameters: exchange interaction J/k_B = 1042 K (positive value represents AFM interaction), alternation parameter α = 0.96, $\chi_{Pauli} = 4.16 \times 10^{-4}$ emu/mol, x = 0.076 and the g-factor $g = 2$ (Fig. 5).

Fig. 6 shows the field dependence of magnetization investigated at different temperatures. No hysteresis was observed in the experimental data. The magnetization at 2 K seems to saturate close to 7 T with value $M_S = 0.135\ N_A\mu_B$ and can be well described by Brillouin function for ideal paramagnet with spin S = 1/2 representing 7% of free spins, similar as value obtained from the temperature dependence of magnetic susceptibility. This analysis confirms very small contribution of strongly-correlated AFM spin dimers formed by TCNQ tetramers to the low-temperature magnetism.

Measurements of EPR spectra of (**1**) (Fig. 7) were realized at operating frequency 9.4 GHz in the temperature range from 2.5 K to room temperature. Resonance line with g-factor $g = 2$ occurs in investigated EPR spectra in the magnetic field range 334–337 mT. The linewidth is decreasing with increasing temperature and the value of linewidth is $\Delta B = 0.54$ mT at temperature 300 K, what is a typical value for TCNQ anion-radicals. The integrated intensity

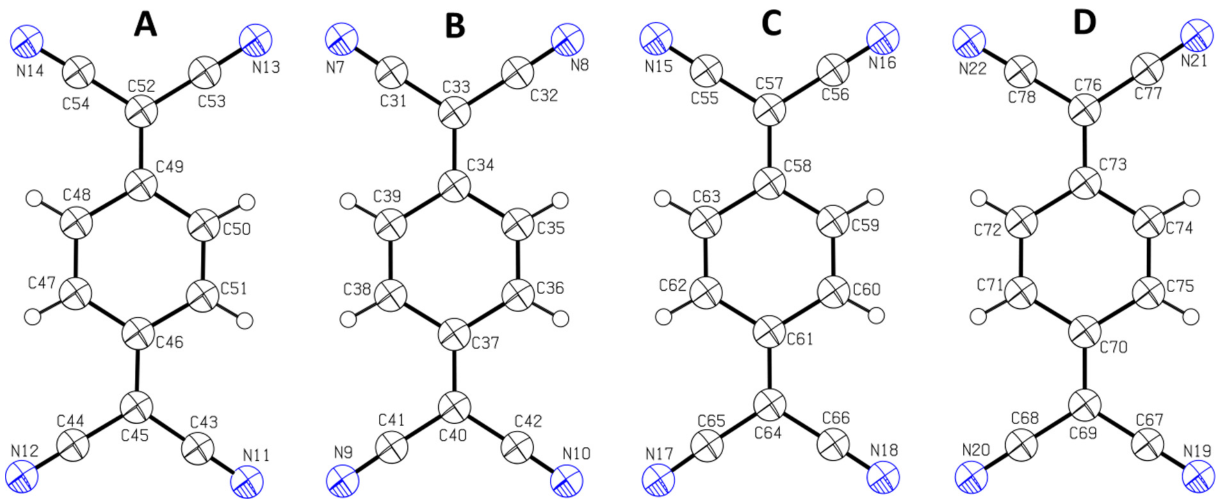

Fig. 3. Molecular structure of TCNQ anion-radicals from asymmetric part of the unit cell of (**3**) according to X-ray diffraction data. Thermal ellipsoids are drawn at 50% probability level.

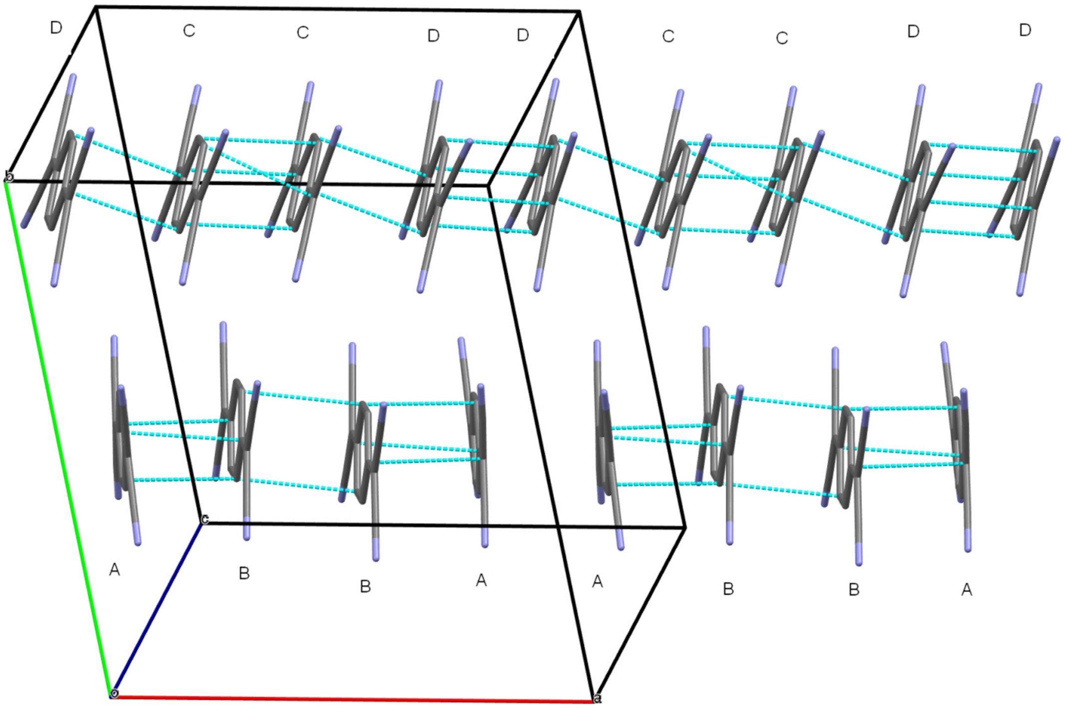

Fig. 4. The tendency for tetramerization (ABBA) and dimerization (CC and DD) of TCNQ stacks in (**3**). Hydrogen atoms are omitted for clarity.

decreases with increasing temperature over the entire temperature range.

As mentioned above, the structures of studied compounds are very similar (same space group, similar cell parameters, but with some small variations of distances between anion radicals) and we use magnetic parameters obtained from the analysis of magnetic properties of (**1**) as the best initial estimate for further analysis of other two studied compounds, where several contributions to the total magnetic moment need to be taken into account.

3.3.2. [Ni(bipy)$_3$](TCNQ)$_4$·(CH$_3$)$_2$CO

Measurement of magnetic susceptibility of (**2**) was carried out at temperatures from 0.46 K to 300 K. The increase of magnetic susceptibility with decreasing temperature was observed in whole studied temperature range (Fig. 8). No difference was observed in the experimental data investigated in ZFC and FC regimes. Effective magnetic moment decreases from value 3.47 μ_B at 300 K to value 2.45 μ_B at 0.46 K. The Ni^{2+} ion in octahedral coordination has spin $S = 1$ with expected value of the effective magnetic moment in paramagnetic limit $\mu_{eff} = 2.83\ \mu_B$. The comparison of theoretical and experimental value of the effective magnetic moment indicates presence of another contribution, which originates from dimerized TCNQ anion-radical chains. The change of the effective magnetic moment is similar to compound (**1**) at higher temperatures and originates from TCNQ stacks. The spins of TCNQ anion-radicals are strongly dimerized at low temperatures and only uncoupled spins and chain ends contribute to the effective magnetic moment as observed in (**1**). Also the field dependence of magnetization measured at 1.8 K shown in Fig. 9 approaches at 7 T a saturation value typical for Ni^{2+} ions.

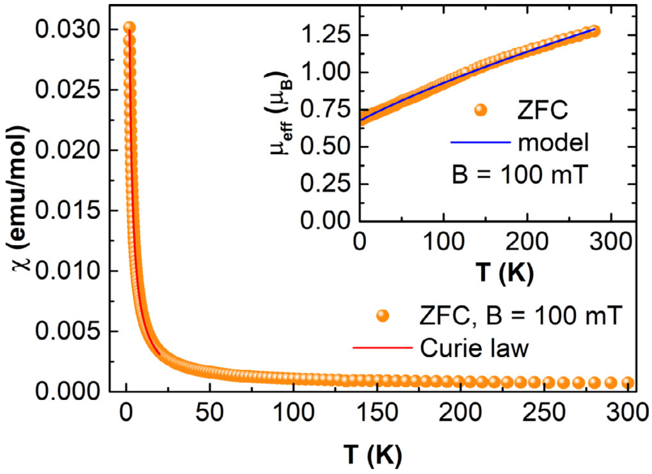

Fig. 5. The low-field magnetic susceptibility of (**1**) plotted as a function of temperature (symbols). The solid line represents Curie law. Inset: The temperature dependence of effective magnetic moment including simulation described in the text.

The temperature dependence of specific heat was investigated in magnetic fields up to 9 T applied parallel to the crystallographic *c*-axis at temperatures from 0.4 K to 30 K. The specific heat of (**2**) in zero magnetic field decreases with decreasing temperature followed by an increase at the lowest temperatures below 2.5 K. After application of external magnetic field, a Schottky-like maximum appears below 10 K. The origin of the maximum in temperature dependence of magnetic specific heat C_{mag} (Fig. 10) was suggested after the subtraction of the phonon contribution C_{latt} from the total specific heat C_{tot}: $C_{mag} = C_{tot} - C_{latt}$ as referred in [22] followed by the determination of magnetic entropy. This study shows that only Ni^{2+} ions contribute to magnetic specific heat at low temperatures.

Low-temperature specific heat of (**2**) was described by the spin Hamiltonian

$$H = D[\mathbf{S}_z^2 - S(S+1)/3] + E(\mathbf{S}_x^2 + \mathbf{S}_y^2) \tag{2}$$

accounting for isolated Ni^{2+} ions with single-ion anisotropy with parameters $D/k_B = -1.95$ K, $E/k_B = 0.3$ K. The overall good agreement of the model with the experimental specific heat considering the mutual orientation of the magnetic-field vector and the easy-axis of the anisotropy is manifested in the Fig. 10 for the higher magnetic fields up to 5 T than reported previously [22]. The obtained negative value of single-ion anisotropy parameter *D* is consistent with the analysis of magneto-structural correlations as described in Ref. [23].

Magnetic susceptibility in the whole temperature range was analyzed by the model accounting for contribution of TCNQ molecules using Eq. (1) with exchange interaction $J/k_B = 1040$ K, alternation parameter $\alpha = 0.96$, $\chi_{Pauli} = 7.6 \times 10^{-4}$ emu/mol, $x = 0.1$ including contribution of Ni^{2+} ions according to Eq. (2) with $D/k_B = -1.95$ K (rhombic parameter *E* was not considered). In addition, a weak AFM exchange interaction between Ni^{2+} ions, $zJ'/k_B = -0.1$ K was considered using molecular-field approximation (Figs. 8–10). While the specific heat simulations include g-factor $g = 2.2$ for Ni^{2+} ions, the simulations of magnetic quantities consider slightly smaller *g*-factor $g = 2.18$. Note that the exchange interaction between Ni^{2+} ions and the contribution of uncoupled TNCQ spins was not included in the simulation of the specific heat.

EPR spectra of (**2**) were investigated at operating frequency 9.4 GHz at different temperatures from 2.2 K to 280 K (Fig. 11). A resonance line appears in magnetic-field range 250 mT–450 mT with *g*-factor $g = 1.95$. Integral intensity of the resonance line decreases up to 50 K and then increases slightly again with increasing temperature, which supports the assumption of the small high-temperature contribution of triplet excitations from dimerized TCNQ chains to the total magnetic moment. This result suggests that the energy gap in the dimerized TCNQ chains may be smaller than in (**1**) and the temperature dependence of the magnetic moment is not enough sensitive to the change of J and α due to the additional contribution of χ_{Pauli}, which does not affect the EPR results.

Table 2
Analysis of the TCNQ bond distances and correlation between bond length and charge of TCNQ molecules.

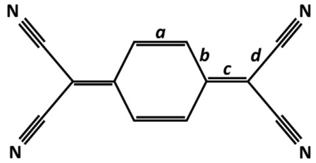

	a	b	c	d	b–c	c–d	c/(b + d)	Q*
$TCNQ^{0}$*	1.345	1.448	1.374	1.441	0.074	–0.067	0.476	0.001
$TCNQ^{-0.5}$*	1.354	1.434	1.396	1.428	0.040	–0.032	0.488	0.500
$TCNQ^{-}$*	1.374	1.423	1.420	1.416	0.003	0.004	0.500	0.999
$[Zn(bipy)_3](TCNQ)_4{\cdot}H_2O$								
TCNQ A	1.354	1.428	1.401	1.414	0.027	–0.013	0.493	0.704
TCNQ B	1.340	1.430	1.402	1.419	0.028	–0.017	0.492	0.673
TCNQ C	1.359	1.427	1.387	1.432	0.0398	–0.045	0.485	0.384
TCNQ D	1.340	1.422	1.398	1.445	0.024	–0.047	0.488	0.480
$[Ni(bipy)_3](TCNQ)_4{\cdot}(CH_3)_2CO$								
TCNQ A	1.348	1.424	1.400	1.421	0.024	–0.026	0.490	0.673
TCNQ B	1.347	1.426	1.392	1.4182	0.033	–0.017	0.492	0.569
TCNQ C	1.350	1.426	1.400	1.415	0.022	–0.015	0.493	0.729
TCNQ D	1.352	1.220	1.401	1.420	0.021	–0.018	0.493	0.715
$[Co(bipy)_3](TCNQ)_4{\cdot}H_2O$								
TCNQ A	1.345	1.426	1.396	1.425	0.030	–0.029	0.490	0.568
TCNQ B	1.349	1.429	1.395	1.426	0.034	–0.031	0.489	0.524
TCNQ C	1.348	1.428	1.395	1.426	0.033	–0.031	0.489	0.530
TCNQ D	1.345	1.424	1.399	1.416	0.024	–0.017	0.493	0.698

* Data and formula taken form Refs. [19,30,31].

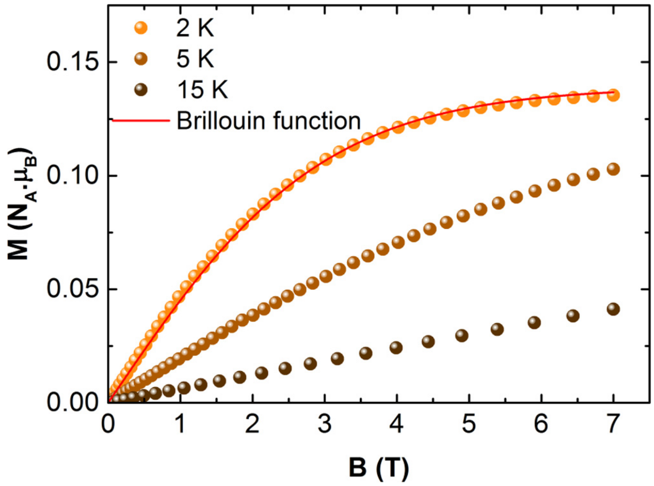

Fig. 6. The field dependence of isothermal magnetization of (**1**) at different temperatures (symbols). The solid line represents a fit using the Brillouin function at 2 K (similar fits were performed at higher temperatures, not shown here).

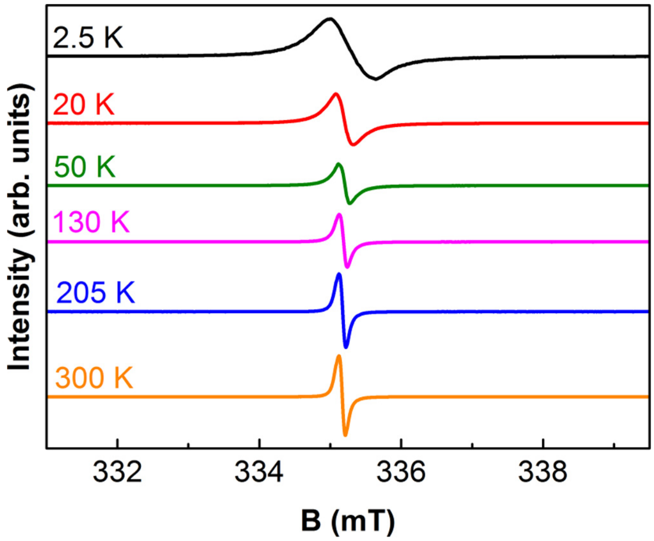

Fig. 7. Temperature evolution of EPR spectra of (**1**).

3.3.3. *[Co(bipy)$_3$](TCNQ)$_4$·H$_2$O*

Magnetic susceptibility of (**3**) was investigated in the temperature range from 4.5 K to 300 K and no difference was observed between measurements in ZFC and FC regimes (Fig. 12). Magnetic susceptibility changes monotonously in the whole temperature range, i.e. increases with decreasing temperature. The effective magnetic moment is $\mu_{eff} = 3.68\ \mu_B$ at 300 K. The obtained value of the effective magnetic moment at room temperature is lower than the theoretical value of $\mu_{eff} = 3.87\ \mu_B$ of Co^{2+} ion in high-spin state with $S = 3/2$ and dramatically different than the value of magnetic moment $\mu_{eff} = 1.73\ \mu_B$ of Co^{2+} ion in a low-spin state with $S = 1/2$. In addition, the effective magnetic moment decreases only very slightly with decreasing temperature to value 3.36 μ_B at 4.5 K. A potential magnetic contribution of spins of TCNQ anion-radicals in ARS (**3**) was assumed to be comparable to that of crystallographic similar ARS (**1**), which contain non-magnetic Zn^{2+} ion. In the temperature dependence of effective magnetic moment in (**3**) the contribution of TCNQ radicals is not clearly evidenced by a gradual increase at higher temperatures (it is present in EPR results discussed below).

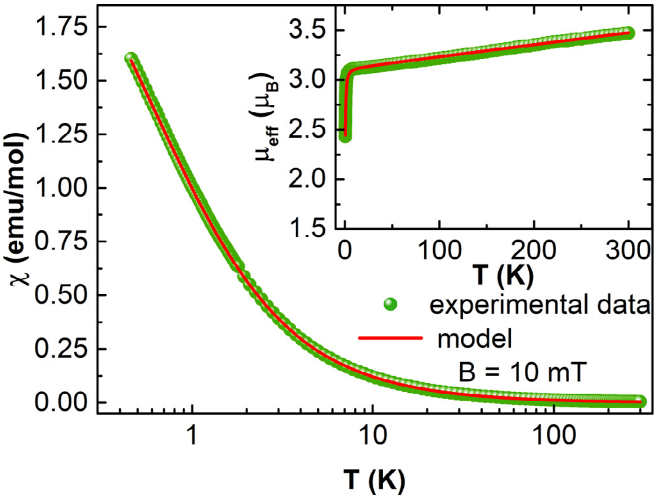

Fig. 8. The magnetic susceptibility of (**2**) (symbols) as a function of temperature in comparison with theoretical model described in the text (solid line). Inset: The temperature dependence of the effective magnetic moment.

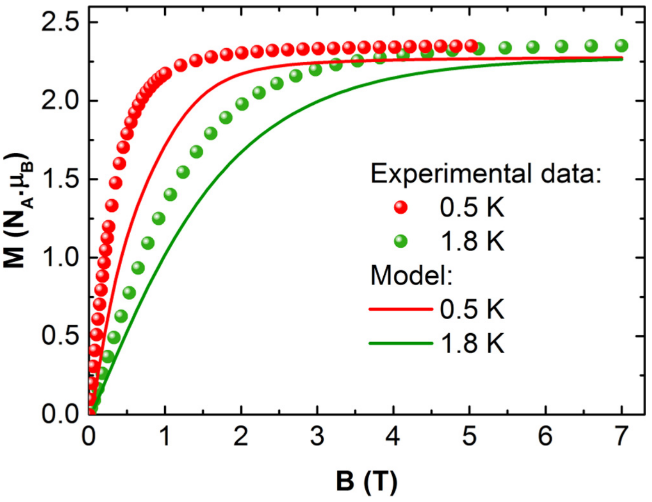

Fig. 9. The field dependence of isothermal magnetization of (**2**) (symbols) plotted along with the results from the simulations described in the text (solid line).

The field dependence of magnetization was measured in the magnetic-field range 0–7 T at temperatures 1.8 K, 5 K and 15 K (Fig. 13) and obtained experimental data do not exhibit any hysteresis. Magnetization saturated to value $M_S = 2.38\ N_A\mu_B$ at 1.8 K. Theoretical values of saturation magnetization for Co^{2+} ion are $M_S = 3\ N_A\mu_B$ in high-spin state and $M_S = 1\ N_A\mu_B$ in low-spin state. The experimental value of saturation magnetization is unusual and does not correspond to the theoretical value for Co^{2+} ions neither in high-spin nor in low-spin state, even after consideration of the magnetic contribution of TCNQ anion-radicals of approximately 0.135 $N_A\mu_B$, based on investigation of (**1**). After subtraction of similar or smaller contribution of TCNQ stacks as in the analogue compound (**1**) from the temperature dependence of the magnetic moment of (**3**) one would observe even slight decrease of the magnetic moment towards the 300 K. Such dependence resembles the one that can be obtained after extrapolation between the high-spin and low-spin state behaviour as shown in Ref. [27] for intermediate crystal-field strength. A plausible explanation is suggested that Co^{2+} ions in (**1**) are in the spin-equilibrium of high-spin and low-spin state. For a certain range of crystal-field strengths a crossover point between $^4T_1(^4F)$ and $^2E(^2G)$ appears and these electronic

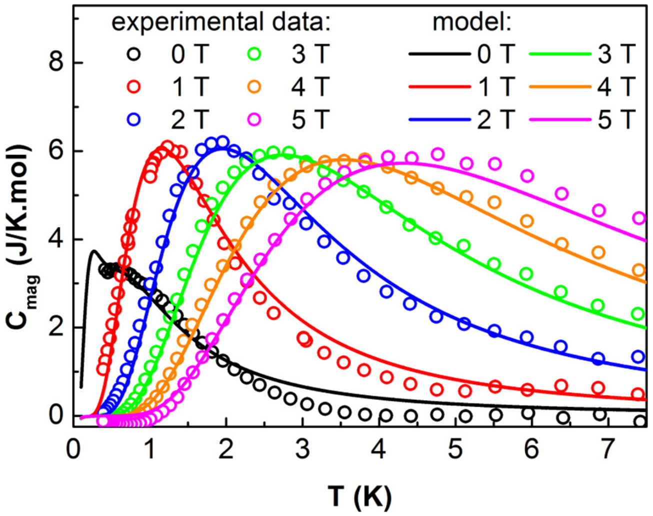

Fig. 10. The comparison of the temperature dependence of magnetic specific heat of (**2**) at different magnetic fields (symbols) with theoretical simulation described in the text (solid lines).

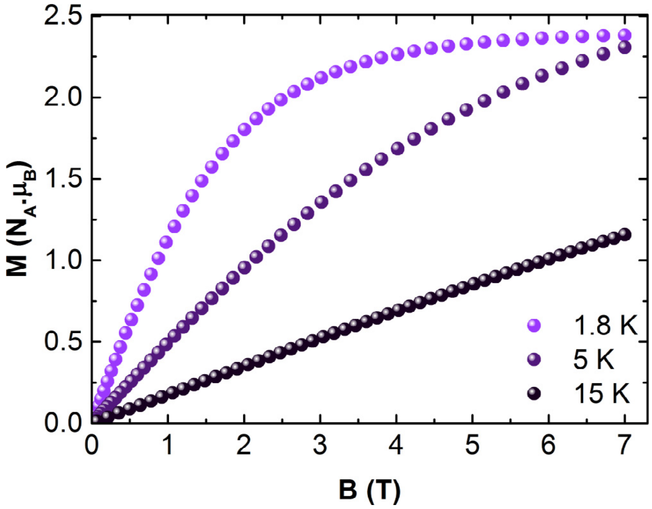

Fig. 13. The field dependence of isothermal magnetization of (**3**) at different temperatures.

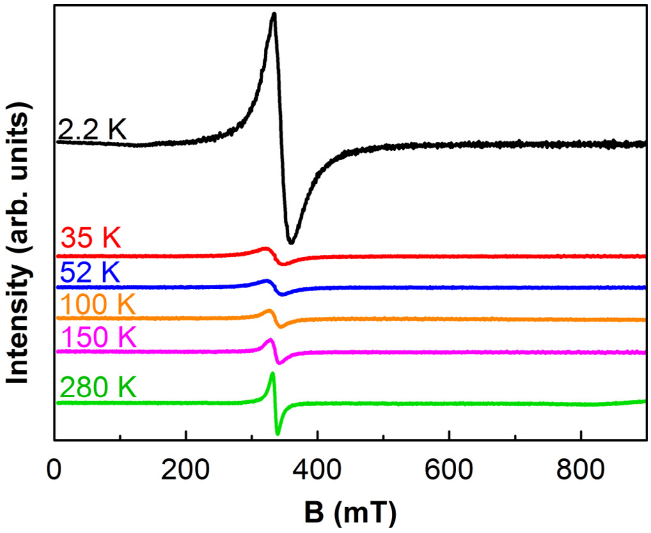

Fig. 11. Temperature evolution of EPR spectra of (**2**).

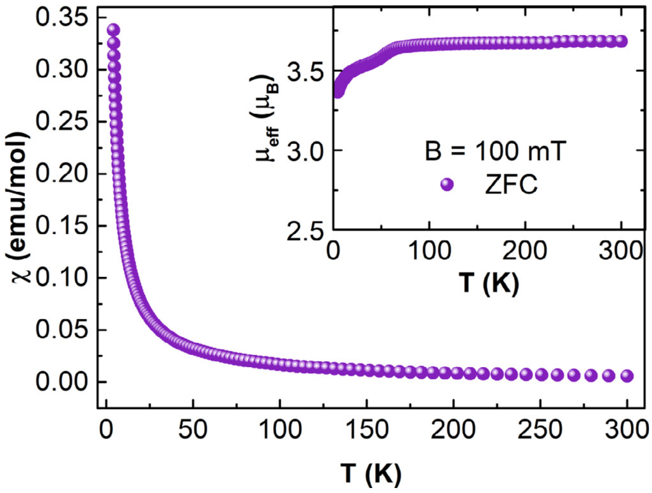

Fig. 12. The low-field magnetic susceptibility of (**3**) plotted as a function of temperature. Inset: The temperature dependence of χT product.

states with different spin multiplicities are mixed [24,25], which is reflected by the value of the effective magnetic moment at room temperature. The states with $M_S = \pm 3/2$ would partially contribute to total magnetic properties, but the resulting magnetic behaviour would not be a simple function of temperature as is predicted by the two-level model. In the result, to obtain the temperature dependence of magnetic moment the calculation in the complete d^7 basis of 120 functions is required. In the case of previously reported compound $[Co(phen)_3](TCNQ)_2\ H_2O$ [11] the high-spin state of Co^{2+} was confirmed despite the phenanthroline is considered as a strong-field ligand. The bipyridine is also considered as a strong-field ligand in the spectrochemical series similar to phenanthroline and we speculate that the differences in the charge distribution at the neighboring TCNQ anion radicals may affect the resulting crystal field at the Co^{2+} site in the compound (**3**) and yield the presence of the spin-admixed state.

In addition, a possible weak exchange interaction between TCNQ anion radicals and Co^{2+} ions mediated by hydrogen bonds as observed in $[Co(phen)_3](TCNQ)_2\ H_2O$ [11] would not significantly reduce the effective magnetic moment from the high-spin value at higher temperature to the one observed in (**3**). Another possible explanation is that the compound exhibits spin-crossover transition. However, the change of the magnetic moment is not so pronounced as expected for fully developed spin-crossover transition and with no thermal hysteresis therefore this interpretation is not probable and EPR measurements also support this idea.

These findings are supported by the measurement of EPR spectra of (**3**) performed at operating frequency 9.4 GHz at different temperatures from 2.1 K to 280 K (Fig. 14). EPR spectra display a broad asymmetric signal with *g*-factor $g = 1.96$ in magnetic field from 250 mT to 470 mT at low temperatures. A resonance line corresponds presumably to indistinguishable spectra of ion Co^{2+} and of anion-radicals TCNQ and close value of their *g*-factors. The value of *g*-factor of ion Co^{2+} is similar to low-spin state of ion Co^{2+} [26,27], but experimental reports [28] and theoretical calculation of *g*-factor for spin-admixed state [25] show the comparable value of *g*-factor. The intensity of the resonance line decreases with increasing temperature up to 75 K. Further increase of temperature above 75 K causes an increase of intensity of the resonance line and change of the resonance line shape to symmetric one. The integral intensity of this signal is decreasing up to 75 K and then increases again with increasing temperature. The increase of intensity with temperature is typical for thermally activated transitions between

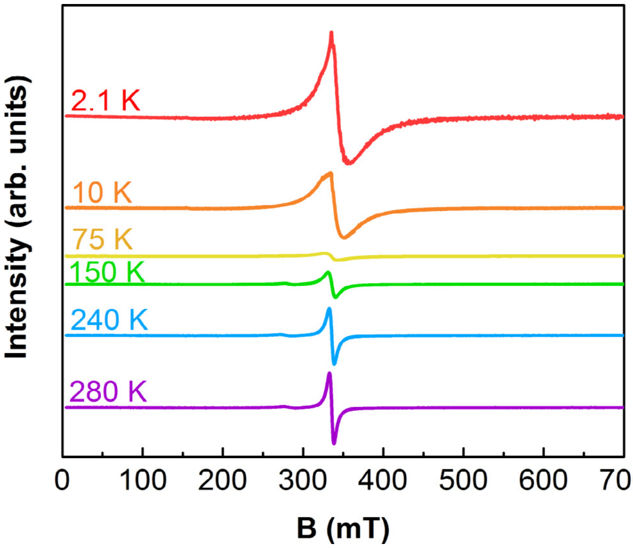

Fig. 14. Temperature evolution of EPR spectra of (**3**).

levels of excited triplets in dimerized spin systems similar to compound (**2**). At temperature 150 K another peak with *g*-factor $g = 2.37$ appears near the central resonance line also observed in systems with Co^{2+} ion in low-spin state [29]. EPR spectra do not exhibit an evidence of the signal in the low-field region related to presence of Co^{2+} in pure high-spin state. A partial contribution of high-spin state of Co^{2+} would probably not be detected because of usually very low signal intensity due to its fast spin-lattice relaxation.

4. Conclusion

In this paper, the results of experimental investigation of ARS $[Zn(bipy)_3](TCNQ)_4\cdot H_2O$, $[Ni(bipy)_3](TCNQ)_4\cdot(CH_3)_2CO$ and $[Co(bipy)_3](TCNQ)_4\cdot H_2O$ by the measurement of the temperature dependence of magnetic susceptibility, the field dependence of magnetization and EPR spectra are presented. All studied ARS are isostructural and contain structural TCNQ tetramers with $S = 0$ ground state (AFM spin dimers with $S = 1/2$). The contribution of uncoupled spins only is observed in magnetic properties in the compound $[Zn(bipy)_3](TCNQ)_4\cdot H_2O$ at low temperatures. An increased population of excited triplet states in dimerized spin chains formed within TCNQ stacks was observed at higher temperatures in the EPR measurements and their contribution to the increase of magnetic moment at higher temperatures is assumed in studied compounds. Low-temperature behaviour of magnetic properties of $[Ni(bipy)_3](TCNQ)_4\cdot(CH_3)_2CO$ can be described using the model including single-ion anisotropy parameters $D/k_B = -1.95$ K, $E/k_B = 0.1$ K and $g = 2.18$ for Ni^{2+} ions and a weak AFM exchange interactions between them. The temperature dependence of specific heat is well described by the same *D* and *E* parameters and $g = 2.2$ in magnetic fields up to 5 T. The compound $[Co(bipy)_3](TCNQ)_4\cdot H_2O$ can be characterized as the system containing Co^{2+} ions in spin-admixed state. This means, this complex appears as one of few compounds, where mixed high-spin and low-spin state is realized.

Acknowledgments

This work was supported by the Slovak Research and Development Agency under contract No. APVV-14-0073 and APVV-0132-11, by ERDF EU projects under the contract Nos. ITMS26220120005, ITMS26220120047, and ITMS26220220186. We thank J. Kuchár for single crystal orientation using X-ray diffraction and prof. M.W. Meisel for the discussion and comments that improved the manuscript. A.V. Fedorchenko thanks P.J. Šafárik University for the opportunity to carry out research.

References

[1] K.P. Goetz, D. Vermeulen, M.E. Payne, Ch. Kloc, LE. McNeilb, O.D. Jurchescu, J. Mater. Chem. C 2 (2014) 3065–3076, https://doi.org/10.1039/C3TC32062F.
[2] V.A. Starodub, T.N. Starodub, Russ. Chem. Rev. 83 (2014) 391–438, https://doi.org/10.1070/RC2014v083n05ABEH004299. and references therein.
[3] R.M. Metzger, J. Mater. Chem. 18 (2008) 4364–4396, https://doi.org/10.1039/b802804b.
[4] S. Bertaina, C.-E. Dutoit, J. van Tol, M. Dressel, B. Barbara, A. Stepanov, Phys. Rev. B 90 (2014) 060404(R), https://doi.org/10.1103/PhysRevB.90.060404.
[5] M. Botko, V.O. Cheranovskii, O.N. Kazheva, G.V. Shilov, O.A. Dyachenko, A.B. Verkin, M. Kucmin, V.A. Starodub, A. Radváková, M. Kajňaková, A. Feher, Solid State Sci. 24 (2013) 85–89, https://doi.org/10.1016/j.solidstatesciences.2013.07.011.
[6] A. Radváková, O.N. Kazheva, A.N. Chekhlov, O.A. Dyachenko, M. Kucmin, M. Kajňáková, A. Feher, V.A. Starodub, J. Phys. Chem. Solids 71 (2010) 752–757, https://doi.org/10.1016/j.jpcs.2010.01.012.
[7] A. Radváková, D.V. Ziolkovskiy, M. Kajňáková, B. Laskowska, B. Barszcz, A. Graja, V.A. Starodub, A. Feher, J. Phys.-Condens. Matter 21 (2009) 175405, https://doi.org/10.1088/0953-8984/21/17/175405.
[8] L. Ballester, A.M. Gil, A. Gutiérrez, M.F. Perpiñán, M.T. Azcondo, A.E. Sánchez, U. Amador, J. Campo, F. Palacio, Inorg. Chem. 36 (1997), https://doi.org/10.1021/ic9703585. 5291–2598.
[9] M. Ballesteros-Rivas, A. Ota, E. Reinheimer, A. Prosvirin, J. Valdes-Martinez, K.R. Dunbar, Angew. Chem. Int. Ed. 50 (2011) 9703–9707, https://doi.org/10.1002/anie.201101658.
[10] C. Alonso, L. Ballester, A. Gutiérrez, M.F. Perpiñán, A.E. Sánchez, M.T. Azcondo, Eur. J. Inorg. Chem. (2005) 486–495, https://doi.org/10.1002/ejic.200400540.
[11] D. Šoltésová, G. Vasylets, E. Čižmár, M. Botko, V. Cheranovskii, V. Starodub, A. Feher, J. Phys. Chem. Solids 99 (2016) 182–188, https://doi.org/10.1016/j.jpcs.2016.08.022.
[12] G.Y. Vasylets, V.A. Starodub, B. Barszcz, A. Graja, V.V. Medviediev, O.V. Shishkina, A.S. Bukrinev, Synth. Met. 191 (2014) 89–98, https://doi.org/10.1016/j.synthmet.2014.02.020.
[13] G.Y. Vasylets, A.V. Khotkevich, A.S. Bukrinev, A.S. Krasnyi, V.A. Starodub, A.A. Kravchenko, V.V. Medviediev, Funct. Mater. 22 (2015) 338–341, https://doi.org/10.15407/fm22.03.338.
[14] G. Sheldrick, Acta Cryst. Sec. A 64 (2008) 112–122, https://doi.org/10.1107/S0108767307043930.
[15] J.C. O'Connor, Magnetochemistry-Advances in Theory and Experimentation, Progress in Inorganic Chemistry, Stephen J. Loppard, NY, 1982.
[16] S. Stoll, A. Schweiger, J. Magn. Reson. 178 (2006) 42, https://doi.org/10.1016/j.jmr.2005.08.013.
[17] www.mathworks.com.
[18] Yu.V. Zefirov, P.M. Zorkiy, Usp. Khim. 58 (1989) 421–440, https://doi.org/10.1070/RC1989v058n05ABEH003451.
[19] T.J. Kistenmacher, T.J. Emge, A.N. Bloch, D.O. Cowan, Acta Crystallogr. Sect. B 38 (1982) 1193–1199, https://doi.org/10.1107/S0567740882005275.
[20] O. Kahn, Molecular Magnetism, VCH Publishers, Inc., NY, 1993.
[21] L. Ballester, A. Gutiérrez, M.F. Perpiñán, A.E. Sánchez, M. Fonari, M. Gdaniec, Inorg. Chem 46 (2007) 946–3955, https://doi.org/10.1021/ic062016h.
[22] D. Šoltésová, E. Čižmár, G. Vasylets, V.A. Starodub, A. Feher, Acta Phys. Pol. A 131 (2017) 925–927, https://doi.org/10.12693/APhysPolA.131.925.
[23] J. Titiš, R. Boča, Ľ. Dlháň, T. Ďurčeková, H. Fuess, R. Ivaniková, V. Mrázová, B. Papánková, I. Svoboda, Polyhedron 26 (2007) 1523–1530, https://doi.org/10.1016/j.poly.2006.11.054.
[24] C. Stoufer, D.W. Smith, E.A. Clevenger, T.E. Norris, Inorg. Chem. 5 (1966) 1167–1171, https://doi.org/10.1021/ic50041a020.
[25] R. Boča, Struct. Bond. 117 (2006) 1–264, https://doi.org/10.1007/b136907.
[26] S.G. Sreerama, D. Shyamraj, S. Pal, S. Pal, Indian J. Chem.-A 42A (2003) 2352–2358.
[27] M.C.R. Symons, T. Taiwo, A.M. Sargeson, M.M. Ali, A.S. Tabl, Inorg. Chim. Acta 241 (1996) 5–8, https://doi.org/10.1016/0020-1693(95)04959-2.
[28] J.G. Schmidt, W.S. Brey Jr., R.C. Stoufer, Inorg. Chem. 6 (1967) 268–271, https://doi.org/10.1021/ic50048a016.
[29] D.W. Shaffer, I. Bhowmick, A.L. Rheingold, C. Tsay, B.N. Livesay, M.P. Shores, J.Y. Yang, Dalton Trans. 45 (2016) 17910–17917, https://doi.org/10.1039/C6DT03461F.
[30] S.Z. Goldberg, R. Eisenberg, J.S. Miller, A.J. Epstein, J. Am. Chem. Soc. 98 (1976) 5173–5182, https://doi.org/10.1021/ja00433a020.
[31] A. Hoeskstra, T. Spoelder, A. Vos, Acta Crystallogr., Sect. B 28 (1972) 14, https://doi.org/10.1107/S0567740872001803.